Guanosine Binds to the *Tetrahymena* Ribozyme in More than One Step, and Its 2′-OH and the Nonbridging *pro*-S_p Phosphoryl Oxygen at the Cleavage Site Are Required for Productive Docking†

Louis A. Profenno,‡ Ryszard Kierzek,§ Stephen M. Testa,‡ and Douglas H. Turner*,‡

Department of Chemistry, Box 270216, University of Rochester, Rochester, New York 14627-0216, and Institute of Bioorganic Chemistry, Polish Academy of Sciences, 60-704 Poznan, Noskowskiego 12/14, Poland

Received April 16, 1997; Revised Manuscript Received August 11, 1997⊗

ABSTRACT: The dynamics of binding of various guanosine, or G, substrates to the *Tetrahymena thermophila* L-21 *Sca*I ribozyme have been investigated by fluorescence-detected stopped-flow experiments. Upon rapid mixing of various G substrates with a preformed complex of the ribozyme and the fluorescent 5′ splice site analogue CCUCUϵA, fluorescence transients that provide rates for binding of G substrates and the rate-limiting step for transesterification are observed. The measured apparent bimolecular rate constant for binding of pG is 10^3 M^{-1} s^{-1}, much slower than expected for diffusion. pG appears to bind to the preformed complex of the ribozyme and CCUCUϵA in at least two steps, a bimolecular step followed by at least one conformational change. This two-step binding of pG, involving a rapid pre-equilibrium, leads to the slow apparent rate constant for binding of pG. Furthermore, the 2′-OH of pG and of the 3′ terminal G of the G substrate GUCG and the nonbridging *pro*-S_p phosphoryl oxygen atom at the site of phosphoryl transfer on CCUCUϵA appear to mediate formation of a properly conformed docked ternary complex of the G substrate, 5′ splice site, and ribozyme which may represent an intermediate required for initiation of transesterification. It is possible that the 2′-OH of pG and this nonbridging *pro*-S_p phosphoryl oxygen interact, directly or indirectly, with one another.

Little is known about the dynamics of natural RNAs in either folding or function. The kinetics of RNA folding have been studied for tRNA (Crothers et al., 1974; Hilbers et al., 1976) and for the *Tetrahymena thermophila* L-21 *Sca*I ribozyme (Zarrinker & Williamson, 1994; Banerjee & Turner, 1995; Sclavi et al., 1997). RNA dynamics related to function have been studied for a spliced leader sequence (Le Cuyer & Crothers, 1994) and for the *Tetrahymena* L-21 *Sca*I ribozyme (Bevilacqua et al., 1992, 1993, 1994; Li et al., 1995; Li & Turner, 1997; Turner et al., 1996). Much remains to be discovered, however, about the factors that affect RNA dynamics.

The *T. thermophila* L-21 *Sca*I ribozyme, R, is a version of the *T. thermophila* LSU intron shortened by 21 and 5 nucleotides at the 5′ and 3′ ends, respectively. It catalyzes a transesterification reaction between an exogenously added analogue of the 5′ splice site and the guanosine, or G, substrate (Inoue & Kay, 1987; Zaug et al., 1988). A 2′-H substitution on G and a sulfur substitution for the nonbridging, *pro*-S_p phosphoryl oxygen atom at the site of transesterification inhibit the transesterification reaction catalyzed by this RNA (Bass & Cech, 1986; Rajagopal et al., 1989; Piccirilli et al., 1993). A mechanism for explaining inhibition by either substitution has not been elucidated, however. An understanding of how these substitutions affect the dynamics of individual steps required for catalysis will offer insights into the catalytic mechanism of RNA.

For either substitution, inhibition could be due to an effect on substrate binding and positioning and/or to an effect on the phosphoryl transfer step. Fluorescent probes of substrate binding and phosphoryl transfer offer a means of following individual steps in the catalytic pathway (Bevilacqua et al., 1992, 1994; Li et al., 1995; Turner et al., 1996) and, therefore, of potentially elucidating how these modifications on substrates affect catalysis. Previous studies have used a pyrene probe at the 5′ end of an oligonucleotide substrate to follow docking of a helix into the catalytic site. As with most fluorescent probes of RNA (Tuschl et al., 1994; Walter & Burke, 1997), the pyrene probe is large, consisting of 38 atoms. Here, we report the application of a much smaller probe, 1,N^6-ethenoadenosine, ϵA (Figure 1) (Tolman et al., 1974; Spencer et al., 1974), to the study of steps involved in the binding of various G substrates to the *T. thermophila* L-21 *Sca*I ribozyme. The ϵA adds only four new atoms to a 5′ splice site analogue and is at the 3′ rather than at the 5′ end of the substrate. A kinetic analysis of interactions between various G substrates and a preformed complex of the 5′ splice site analogue CCUCUϵA, and its phosphorothioate derivatives, with the L-21 *Sca*I ribozyme has been undertaken. Changes in the environment of ϵA lead to changes in ϵA fluorescence (Tolman et al., 1974; Spencer et al., 1974; Kubota et al., 1983). Herein, fluorescence transients are shown to result upon binding of the G substrate to the complex of the ribozyme and CCUCUϵA. By analyzing the fluorescence transients induced by different G substrates, we infer that the G substrate binds in at least two steps to the complex of the ribozyme and CCUCUϵA and that the 2′-OH of the G substrate and the nonbridging, *pro*-S_p phosphoryl oxygen at the site of phosphoryl transfer

† This work was supported by NIH Grant GM22939.
* To whom correspondence should be addressed.
‡ University of Rochester.
§ Polish Academy of Sciences.
⊗ Abstract published in *Advance ACS Abstracts,* September 15, 1997.

S0006-2960(97)00889-1 CCC: $14.00

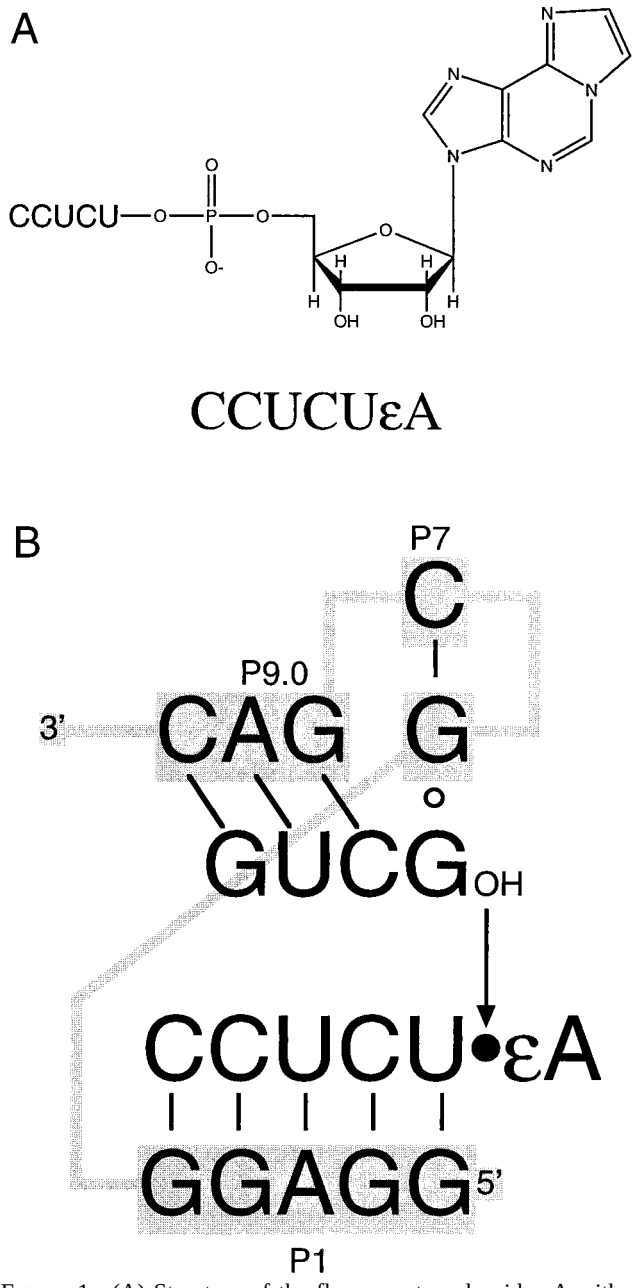

FIGURE 1: (A) Structure of the fluorescent nucleoside ϵA with a phosphodiester linkage to CCUCU. One or the other of the nonbridging phosphoryl oxygen atoms shown is replaced by a sulfur atom in the *pro-*R_p or *pro-*S_p phosphorothioate. All other phosphate linkages in these sulfur-substituted substrates are phosphodiesters. (B) Schematic of the secondary structure of the active site of L-21 *Sca*I (Michel & Westhof, 1990) with CCUCUϵA and GUCG substrates bound. Shaded lines and nucleotides represent the ribozyme sequence. Black lines represent base pairing between substrates and the ribozyme and between nucleotides G249 and C311 of the ribozyme. CCUCUϵA binds to GGAGG (shaded), a part of the internal guide sequence of the ribozyme, to form helix P1. GUC of GUCG binds to CAG (shaded) to form an extended helix P9.0. The open circle represents a base triplet formed between the 3′ terminal G of GUCG and the G249•C311 base pair of the ribozyme. The closed circle represents the phosphate bond of substrate attacked by the 3′-OH of the 3′ terminal G of GUCG during the phosphoryl transfer reaction.

are important for productive alignment of CCUCUϵA in the ternary complex prior to transesterification.

MATERIALS AND METHODS

Materials. The L-21 *Sca*I ribozyme was prepared as previously described (Bevilacqua et al., 1994). pG and pdG were obtained from Sigma. Oligonucleotides except CCUCUϵA and GUC3′dG were synthesized and purified as previously described (Bevilacqua et al., 1994). CCUCUϵA, with and without a thio substitution, and GUC3′dG were prepared using tetrahydropyranyl as the 2′-O blocking group (Markiewicz et al., 1984; Iyer et al., 1990; Stec et al., 1984). For thio-substituted CCUCUϵA, the *pro-*R_p and *pro-*S_p diastereomers were separated and purified by HPLC using a Supelcosil ABZ+Plus column and an isocratic mobile phase of 100 mM TEAA/15% acetonitrile in H_2O. The substrate was characterized as a *pro-*R_p or *pro-*S_p phosphorothioate as described by Weeks and Cech (1995).

Prior to experiments, GUC3′dG and GUCdG were pretreated with 4 mM sodium periodate for 1 h at room temperature to convert the *cis*-diol of any ribo-G contaminant to an unreactive dialdehyde form (Kay & Inoue, 1987). This was done to ensure that fluorescence transients observed with GUC3′dG and GUCdG were not due to ribose contaminants. To inactivate the periodate, 20 mM ethylene glycol was added, and this mixture was allowed to react for 1 h at room temperature. Control experiments with GUCG demonstrated that this procedure eliminates the fluorescence transients associated with the binding of and transesterification with GUCG. Also, further control experiments with GUCG demonstrated that the presence of ethylene glycol and inactivated sodium periodate causes no changes in fluorescence traces produced upon mixing GUCG with a complex of the ribozyme and CCUCUϵA.

Kinetics. All kinetics experiments were performed at 15 °C in 5 mM $MgCl_2$, 110 mM NaCl, and 50 mM NaHEPES at pH 7.5. The ribozyme was renatured in this solution by incubating for 10 min at 50 °C and cooling to room temperature.

In stopped-flow mixing experiments, a preformed complex of the ribozyme and CCUCUϵA was mixed with the G substrate in a KinTek stopped-flow apparatus with a 1.5 ms mixing time (Johnson, 1986), a 395 nm band-pass filter (50 nm FWHM), and a 75 W xenon lamp. A solution containing 400 or 800 nM ribozyme and 400 nM CCUCUϵA was equilibrated for 10 min at 15 °C prior to mixing with the G substrate. After mixing, it is estimated that greater than 87% of the premixed ribozyme and CCUCUϵA exists as a base-paired complex, R•CCUCUϵA (Bevilacqua et al., 1994). Doubling the concentration of the ribozyme or CCUCUϵA does not alter measured rates, confirming that duplex formation does not contribute to the rates. Concentrations of the G substrate were in at least 10-fold excess of that of the R•CCUCUϵA complex to maintain pseudo-first-order conditions. Excitation of samples was at 280 or 310 nm. Excitation at 280 and 310 nm enhances the fluorescence signal at lower and higher concentrations, respectively, of pG or GUCG. Rates are independent of excitation wavelength. For each fluorescence trace, 500 data points were collected. For some traces, data were collected in two time domains with 250 data points in each. All rates are from an exponential fit of an average of several individual traces, and errors are the standard error of this fit. The axis of fluorescence intensity, measured in volts (V), for each trace presented has been offset by subtracting a constant from the real voltage of each trace in order to give an origin of 0 V. This allows easier comparison of the amplitudes for various traces.

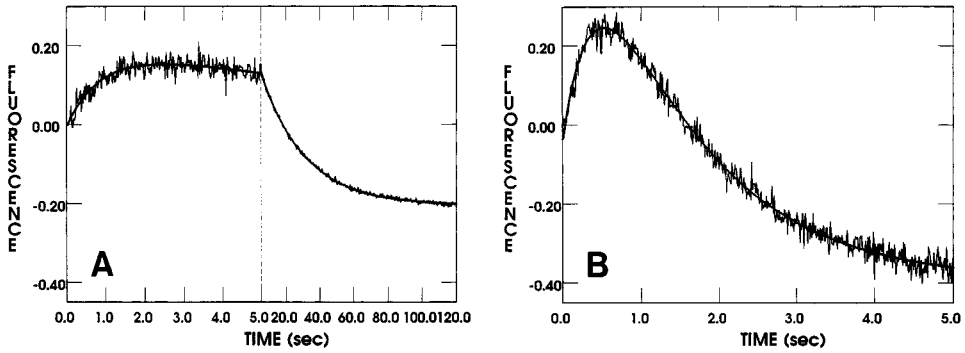

FIGURE 2: (A) Representative trace and exponential fit for the dependence of fluorescence intensity on time after mixing equal volumes of 400 nM CCUCUϵA/400 nM ribozyme and 1 mM pG. Excitation was at 280 nm. The trace represents an average of three individual traces. The trace is fit to $Y = A_1e^{-k_1t} + A_2e^{-k_2t} + C$. The observed rate constant of enhancement is 1.14 ± 0.05 s^{-1}, and the amplitude of enhancement is -0.205 ± 0.004 V. The observed rate constant of quenching is 0.039 ± 0.001 s^{-1}, and the amplitude of quenching is 0.408 ± 0.002 V. Errors are standard errors. $C = -0.205$ V. χ^2 is 0.0885. The trace is offset to give an origin of 0 V as explained in Materials and Methods. In the original averaged trace, the initial voltage equals 5.109 V. The dashed line represents division of trace into two time domains as explained in the methods section. (B) Representative trace and exponential fit for the dependence of fluorescence intensity on time after mixing equal volumes of 400 nM CCUCUϵA/400 nM ribozyme and 100 μM GUCG. Excitation was at 280 nm. The trace represents an average of three individual traces. The trace is fit to $Y = A_1e^{-k_1t} + A_2e^{-k_2t} + C$. The observed rate constant of enhancement is 2.48 ± 0.13 s^{-1}, and the amplitude of enhancement is -0.96 ± 0.07 V. The observed rate constant of quenching is 0.73 ± 0.03 s^{-1}, and the amplitude of quenching is 1.34 ± 0.06 V. Errors are standard errors. $C = -0.396$ V. χ^2 is 0.234. The trace is offset to give an origin of 0 V as explained in Materials and Methods. In the original averaged trace, the initial voltage equals 6.859 V.

Fluorescence-detected stopped flow was similarly utilized to analyze complex formation between the ribozyme and CCUCUϵA or its thioate derivatives. For these experiments, 100 nM ribozyme was mixed with CCUCUϵA ranging in concentration from 200 to 800 nM. Fluorescence data were collected and analyzed as previously described. Excitation of samples was at 280 nm.

Rates for transesterification with CCUCUϵA labeled at the 5′ end with ^{32}P were measured by hand mixing. Similar concentrations of pG and a preformed complex of the ribozyme and CCUCUϵA were used as in the stopped-flow experiments. Reaction time points were collected by removing aliquots and quenching them in an equal volume of stop buffer (10 M urea, 3 mM EDTA, and 0.1× TBE). The reaction components were separated on a 20% acrylamide/8 M urea gel, and bands were quantified on a Molecular Dynamics phosphorimager. Typically, 10 time points were collected over at least 3 half-lives of a given reaction. For each experiment, the percent of CCUCUϵA cleaved as a function of time was fit to a single exponential using the SigmaPlot fitting program (Jandel) to yield an observed rate constant for transesterification. Standard errors in fitting were less than 10%, and each reported observed rate constant represents an average of values from two independent experiments.

For the *pro-S$_p$* phosphorothioate substrate, Mn^{2+} rescue of substrate binding conformation and transesterification were monitored by fluorescence-detected stopped-flow and gel electrophoresis, respectively, as previously described. However, for these experiments, a mixture of 1 mM $MnCl_2$ and 4 mM $MgCl_2$ was substituted for 5 mM $MgCl_2$.

RESULTS

Mixing of a Preformed Complex of the Ribozyme and CCUCUϵA with pG Yields Two Fluorescence Transients with Rates for Two-Step Binding of pG and the Rate-Limiting Step for Transesterification. Mixing of a preformed complex of the ribozyme and CCUCUϵA with pG produces two fluorescence transients, an enhancement and a subsequent quenching of fluorescence (Figure 2A). Fluorescence traces fit a double-exponential function yielding observed rate constants for each transient. The fluorescence quenching exhibits an increase in rate with increasing concentrations of pG. This rate presumably reports the rate of the rate-limiting step for transesterification because the observed rate constant of quenching, 0.06 s^{-1}, at saturating concentrations of 5 mM pG is consistent with the rate for transesterification, 0.06 s^{-1}, measured for CCUCUϵA with a ^{32}P assay (data not shown) and with the previously reported rates of 0.04 and >0.05 s^{-1} for transesterification of pyrene-CCUCUA and CCUCUA substrates, respectively, under the same conditions (Bevilacqua et al., 1994). Therefore, the quenching of fluorescence is assigned either to a conformational rearrangement concomitant with or to a step (e.g. release of pGϵA) after and much faster than the rate-limiting step for transesterification. pdG does not produce this quenching transient, although it does bind to the ribozyme (Moran et al., 1993). That pdG does not undergo transesterification (Bass & Cech, 1986) is also consistent with the quenching being associated with transesterification. The fluorescence enhancement precedes quenching and also exhibits an increase in rate with increasing concentrations of pG. Therefore, the enhancement reflects binding of pG to the R·CCUCUϵA complex or subsequent conformational changes of the pG·R·CCUCUϵA ternary complex.

The rates of both fluorescence transients exhibit hyperbolic dependencies on pG concentration (see the Supporting Information). This is consistent with a minimal three-step reaction mechanism:

Scheme 1

$$\text{pG} + \text{R•CCUCU}\epsilon\text{A} \underset{k_{-1}}{\overset{k_1}{\rightleftharpoons}} \text{pG•R•CCUCU}\epsilon\text{A} \underset{k_{-2}}{\overset{k_2}{\rightleftharpoons}} [\text{pG•R•CCUCU}\epsilon\text{A}]' \underset{k_{-c}}{\overset{k_c}{\rightleftharpoons}} \text{pG}\epsilon\text{A•R•CCUCU}$$

Here, binding of pG occurs in two steps, and the first step, or the bimolecular step, is not observed by stopped flow.

For the mechanism of Scheme 1 with the first step being a rapid preequilibrium, and τ_e^{-1} and τ_q^{-1} being the observed rate constants for enhancement and quenching, respectively (Bernasconi, 1976):

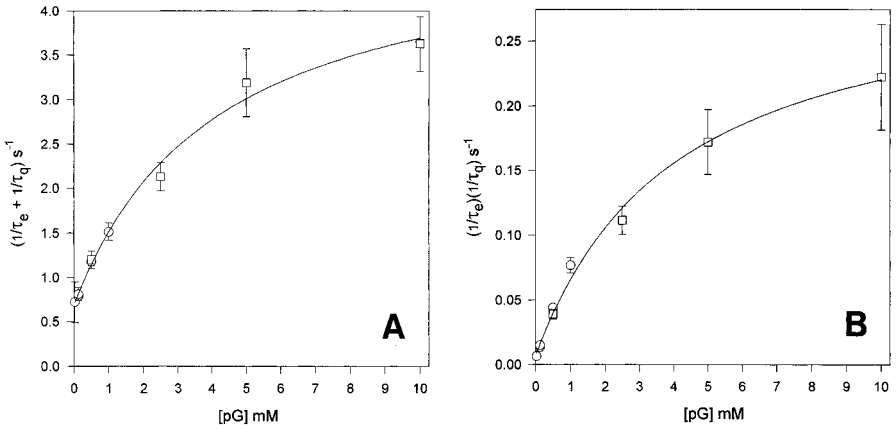

FIGURE 3: (A) Dependence of the sum of observed rate constants of fluorescence enhancement and quenching, $\tau_e^{-1} + \tau_q^{-1}$, on concentration of pG. The solid line represents a hyperbolic fit of data to eq 1 (see the text). χ^2 for this fit is 0.0273, while χ^2 for a linear fit is 0.531. Excitation was at (○) 280 and (□) 310 nm. Error bars on data points represent the standard error of the sum. (B) Dependence of the product of observed rate constants of fluorescence enhancement and quenching, $\tau_e^{-1}\tau_q^{-1}$, on concentration of pG. The solid line represents a hyperbolic fit of data to eq 2 (see the text). χ^2 for this fit is 0.004 25, while χ^2 for a linear fit is 0.0723. Excitation was at (○) 280 and (□) 310 nm. Error bars on data points represent the standard error of the product.

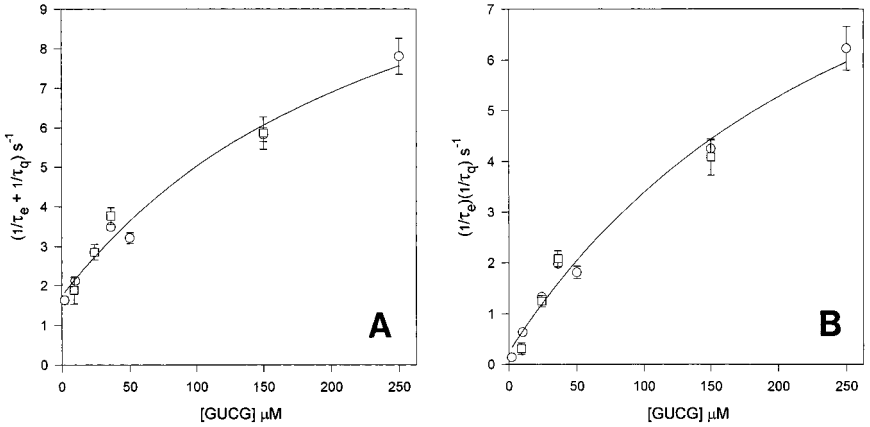

FIGURE 4: (A) Dependence of the sum of observed rate constants of fluorescence enhancement and quenching, $\tau_e^{-1} + \tau_q^{-1}$, on concentration of GUCG. The solid line represents a hyperbolic fit of data to eq 1 (see the text). χ^2 for this fit is 0.283, while χ^2 for a linear fit is 0.580. Excitation was at (○) 280 and (□) 310 nm. Error bars on data points represent the standard error of the sum. (B) Dependence of the product of observed rate constants of fluorescence enhancement and quenching, $\tau_e^{-1}\tau_q^{-1}$, on concentration of GUCG. The solid line represents a hyperbolic fit of data to eq 2 (see the text). χ^2 for this fit is 0.600, while χ^2 for a linear fit is 1.275. Excitation was at (○) 280 and (□) 310 nm. Error bars on data points represent the standard error of the product.

$$\tau_e^{-1} + \tau_q^{-1} = \{(k_2k_1/k_{-1})[\text{G cofactor}]/ [1 + (k_1/k_{-1})[\text{G cofactor}]]\} + k_{-2} + k_c + k_{-c} \quad (1)$$

$$\tau_e^{-1}\tau_q^{-1} = \{(k_2k_1/k_{-1})(k_c + k_{-c})[\text{G cofactor}]/ [1 + (k_1/k_{-1})[\text{G cofactor}]]\} + k_{-2}k_{-c} \quad (2)$$

Figure 3 shows plots of $\tau_e^{-1} + \tau_q^{-1}$ and $\tau_e^{-1}\tau_q^{-1}$ as a function of pG concentration. A fit to eq 1 of the plot of $\tau_e^{-1} + \tau_q^{-1}$ vs [pG] (Figure 3A) gives values for $k_{-2} + k_c + k_{-c}$ of 0.69 ± 0.06 s^{-1}, k_2k_1/k_{-1} of 1030 ± 143 M^{-1} s^{-1}, and k_1/k_{-1} of 243 ± 48 M^{-1}. A fit to eq 2 of the plot of $\tau_e^{-1}\tau_q^{-1}$ vs [pG] (Figure 3B) gives values for $(k_2k_1/k_{-1})(k_c + k_{-c})$ of 74 ± 9 M^{-1} s^{-1}, k_1/k_{-1} of 245 ± 41 M^{-1}, and $k_{-2}k_{-c}$ of 0.007 ± 0.004 s^{-1}. This allows calculation of the following quantities: $k_2 = 4.2 \pm 1.0$ s^{-1}, $k_{-2} = 0.62 \pm 0.06$ s^{-1}, $k_c + k_{-c} = 0.07 \pm 0.01$ s^{-1}, and dissociation constants $K_{d,1} = k_{-1}/k_1$ of 4.1 ± 0.8 mM and $K_d = k_{-1}k_{-2}/k_1k_2$ of 599 ± 104 μM for the first step and both steps, respectively, in the binding of pG. The rate constant for binding is an apparent rate constant, $k_{on,app} = k_2k_1/k_{-1}$, and the limiting rate constant for dissociation is k_{-2}. The calculated K_d is close in value to the value of 1.5 mM measured by Moran et al. (1993).

The dynamics of GUCG binding are consistent with Scheme 1. Figure 2B shows a typical plot of fluorescence intensity vs time after mixing a preformed R·CCUCUϵA complex with GUCG. The observed rate constants of fluorescence enhancement and quenching as a function of GUCG concentration are shown in the Supporting Information, and plots of $\tau_e^{-1} + \tau_q^{-1}$ and $\tau_e^{-1}\tau_q^{-1}$ vs [GUCG] are shown in Figure 4. Fits to eqs 1 and 2 give the following rate and dissociation constants: $k_2 = 12 \pm 7$ s^{-1}, $k_{-2} = 0.81 \pm 0.39$ s^{-1}, $k_c + k_{-c} = 0.9 \pm 0.3$ s^{-1}, $k_{on,app} = k_2k_1/k_{-1} = 4.5 \times 10^4 \pm 1.1 \times 10^4$ M^{-1} s^{-1}, $K_{d,1} = 270 \pm 130$ μM, and $K_d = 18 \pm 10$ μM. This K_d is similar to the value of 6.6 μM measured by Moran et al. (1993). The 40-fold faster rate constant, $k_{on,app}$, for binding of GUCG relative to that of pG could result from a larger actual bimolecular association rate constant, k_1, for the first step in binding, a larger forward rate constant, k_2, for the second step in binding, or the expected slower dissociation rate constant, k_{-1}, of the collision complex resulting from additional base-pairing interactions (see Figure 1), or some combination of these effects. The similarity of the k_{-2} values for pG and GUCG is consistent with release of both substrates being limited by a similar conformational rearrangement of the ternary

Table 1: Summary of Rate and Dissociation Constants for Various G Substrates

G substrate	$k_{on,app}$[b] (M^{-1} s^{-1})	k_2 (s^{-1})	k_{-2} (s^{-1})	$K_{d,1}$[c] (μM)	K_d[d] (μM)	$k_c + k_{-c}$ (s^{-1})
pG[a]	1030 ± 143	4.2 ± 1.0	0.62 ± 0.06	4100 ± 800	599 ± 104	0.07 ± 0.01
GUCG[a]	45 000 ± 11 000	12 ± 7	0.81 ± 0.39	270 ± 130	18 ± 10	0.9 ± 0.3
		k_{on} (M^{-1} s^{-1})		k_{off} (s^{-1})		K_d (μM)
GUCdG		82 000 ± 5000		1.1 ± 0.3		13 ± 4
GUC3′dG		37 000 ± 4000		4.1 ± 0.4		110 ± 20

[a] Rate and dissociation constants refer to Scheme 1 (see the text) describing a mechanism for G substrate binding and were derived from fits of rate data to eqs 1 and 2 (see the text). [b] $k_{on,app} = k_2k_1/k_{-1}$. [c] $K_{d,1}$ ($=k_{-1}/k_1$) is the dissociation constant for the first step only in G substrate binding. [d] K_d ($=k_{-1}k_{-2}/k_1k_2$) is the overall dissociation constant for both steps in G substrate binding.

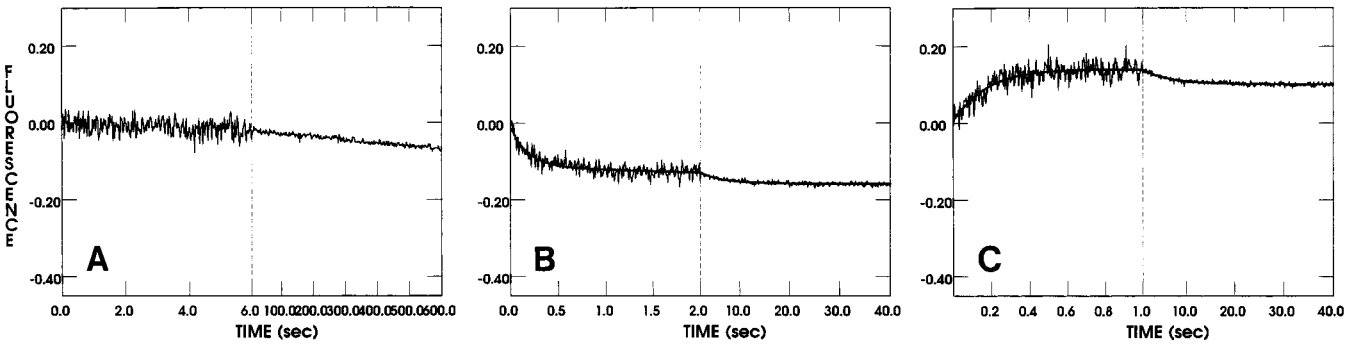

FIGURE 5: (A) Representative trace for the dependence of fluorescence intensity on time after mixing equal volumes of 400 nM CCUCUϵA/400 nM ribozyme and 1 mM pdG. Excitation was at 280 nm. The trace represents an average of two individual traces. The trace is offset to give an origin of 0 V as explained in Materials and Methods. In the original averaged trace, the initial voltage equals 5.378 V. The dashed line represents the division of the trace into two time domains as explained in Materials and Methods. (B) Representative trace and exponential fit for the dependence of fluorescence intensity on time after mixing equal volumes of 400 nM CCUCUϵA/400 nM ribozyme and 100 μM GUCdG. Excitation was at 280 nm. The trace represents an average of seven individual traces. The trace is fit to $Y = A_1e^{-k_1t} + A_2e^{-k_2t} + C$. The observed rate constant of the first quenching phase is 5.46 ± 0.46 s^{-1}, and the amplitude of this phase is 0.098 ± 0.005 V. The observed rate constant of the second quenching phase is 0.214 ± 0.029 s^{-1}, and the amplitude of quenching is 0.045 ± 0.002 V. Errors are standard errors. $C = -0.158$ V. χ^2 is 0.0572. The trace is offset to give an origin of 0 V as explained in Materials and Methods. In the original averaged trace, the initial voltage equals 5.233 V. (C) Representative trace and exponential fit for the dependence of fluorescence intensity on time after mixing equal volumes of 400 nM CCUCUϵA/400 nM ribozyme and 100 μM GUC3′dG. Excitation was at 280 nm. The trace represents an average of five individual traces. The trace is fit to $Y = A_1e^{-k_1t} + A_2e^{-k_2t} + C$. The observed rate constant of enhancement is 5.51 ± 0.39 s^{-1}, and the amplitude of enhancement is −0.139 ± 0.005 V. The observed rate constant of quenching is 0.177 ± 0.031 s^{-1}, and the amplitude of quenching is 0.046 ± 0.003 V. Errors are standard errors. $C = 0.082$ V. χ^2 is 0.119. The trace is offset to give an origin of 0 V as explained in Materials and Methods. In the original averaged trace, the initial voltage equals 4.956 V.

complex, as expected for the mechanism in Scheme 1. Table 1 summarizes rate and dissociation constants for these G substrates.

2′-H and 3′-H Substitutions on the G Substrate Result in Changes in the Fluorescence Traces, Suggesting Changes in Binding. The enhancement and quenching of fluorescence observed upon mixing pG or GUCG with a preformed complex of the ribozyme and CCUCUϵA are not produced with pdG (Figure 5A) or GUCdG (Figure 5B). With pdG, no significant transient is observed, even though pdG is known to bind to the ribozyme with a K_d similar to that of pG (Moran et al., 1993). This suggests the initial binding of pG does not result in a fluorescence change, as discussed above. GUCdG produces a quenching of fluorescence attributable to its binding. The quenching fits a double-exponential function with the amplitude of the faster exponential opposite in sign from and about 10-fold less than that observed for the fluorescence enhancement associated with binding of GUCG. Pretreatment of the GUCdG with sodium periodate does not lead to significant changes in the fluorescence traces, ruling out reaction with a ribo-G contaminant as a source for the quenching. The rate of the faster exponential increases with GUCdG concentration (Figure 6) and is attributed to binding of GUCdG to the R·CCUCUϵA complex. For the slower exponential, rates and amplitudes are similar to those observed with controls in which a preformed R·CCUCUϵA complex is mixed with buffer. Therefore, this phase of the fluorescence quenching is likely due to a small amplitude mixing artifact at long times. The results in Figure 6 are consistent with either one- or two-step binding of GUCdG. For this case, the observed rate constant, τ^{-1}, is given by Bernasconi (1976):

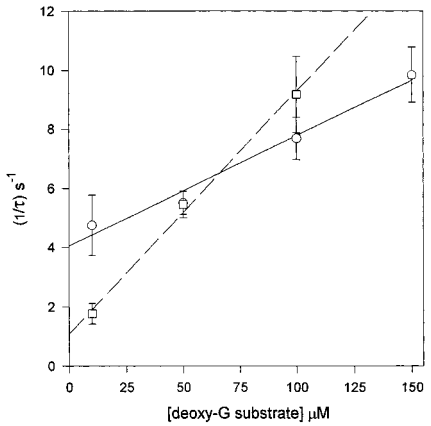

FIGURE 6: Dependence of the observed rate constant of fluorescence transient (τ^{-1}), as described in the text, on concentration of GUCdG (□) and GUC3′dG (○). The solid line represents a linear fit of data for GUC3′dG, and the dashed line represents a linear fit of data for GUCdG. Error bars represent the standard error of the rate.

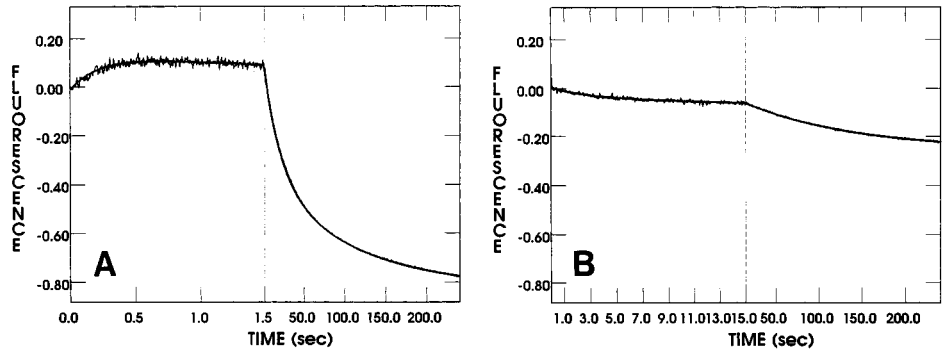

FIGURE 7: (A) Representative trace and exponential fit for the dependence of fluorescence intensity on time after mixing equal volumes of 800 nM CCUCUϵA/400 nM ribozyme and 10 mM pG. The CCUCUϵA contains a *pro-*R_p thio substitution as described in the text. Excitation was at 310 nm. The trace represents an average of three individual traces. The trace is fit to $Y = A_1e^{-k_1t} + A_2e^{-k_2t} + A_2e^{-k_3t} + C$. The observed rate constant of enhancement is 4.62 ± 0.18 s^{-1}, and the amplitude of enhancement is −0.143 ± 0.003 V. The observed rate constants of quenching are 0.0478 ± 0.0018 and 0.008 82 ± 0.000 70 s^{-1} with amplitudes of 0.500 ± 0.021 and 0.460 ± 0.013 V, respectively. Errors are standard errors. $C = -0.830$ V. χ^2 is 0.0398. The trace is offset to give an origin of 0 V as explained in Materials and Methods. In the original averaged trace, the initial voltage equals 5.878 V. The dashed line represents the division of the trace into two time domains as explained in Materials and Methods. (B) Representative trace and exponential fit for the dependence of fluorescence intensity on time after mixing equal volumes of 800 nM CCUCUϵA/400 nM ribozyme and 10 mM pG. The CCUCUϵA contains a *pro-*S_p thio substitution as described in the text. Excitation was at 310 nm. The trace represents an average of two individual traces. The trace is fit to $Y = A_1e^{-k_1t} + A_2e^{-k_2t} + C$. Observed rate constants of quenching are 0.386 ± 0.026 and 0.007 87 ± 0.000 17 s^{-1} with amplitudes of 0.0409 ± 0.0014 and 0.219 ± 0.002 V, respectively. Errors are standard errors. $C = -0.256$ V. χ^2 is 0.0102. The trace is offset to give an origin of 0 V as explained in Materials and Methods. In the original averaged trace, the initial voltage equals 5.394 V. The dashed line represents the division of the trace into two time domains as explained in Materials and Methods.

$$\tau^{-1} = k_{on}[\text{GUCdG}] + k_{off} \quad (3)$$

For one-step binding, $k_{on} = k_1$ and $k_{off} = k_{-1}$; for two-step binding, $k_{on} = k_2k_1/k_{-1}$ and $k_{off} = k_{-2}$. A fit of the data to eq 3 yields a k_{on} of $8.2 \times 10^4 \pm 0.5 \times 10^4$ M^{-1} s^{-1} and a k_{off} of 1.1 ± 0.3 s^{-1}. The dissociation constant, $K_d = k_{off}/k_{on}$, equals 13 ± 4 μM for GUCdG.

Mixing of GUC3′dG with a preformed complex of the ribozyme and CCUCUϵA produces an enhancement of fluorescence followed by a smaller, slower quenching of fluorescence (Figure 5C). The rate and amplitude of the enhancement are not significantly changed with sodium periodate pretreatment of the GUC3′dG, indicating that GUC3′dG rather than a ribo-G contaminant is responsible for the fluorescence enhancement. The rate and amplitude of the fluorescence quenching are similar to those obtained when a preformed R·CCUCUϵA complex is mixed with buffer. Therefore, this fluorescence quenching also is probably due to a small amplitude mixing artifact at long times. The rate of the enhancement increases with concentration of GUC3′dG (Figure 6) and is attributed to binding of GUC3′dG to the complex of the ribozyme and CCUCUϵA. A fit of the data to eq 3 yields a k_{on} of $3.7 \times 10^4 \pm 0.4 \times 10^4$ M^{-1} s^{-1} and a k_{off} of 4.1 ± 0.4 s^{-1}. The dissociation constant, $K_d = k_{off}/k_{on}$, equals 110 ± 20 μM for GUC3′dG. Table 1 summarizes rate and dissociation constants for these deoxy-G substrates.

A Thio Substitution for the pro-S_p *Nonbridging Phosphoryl Oxygen Atom at the Site of Phosphoryl Transfer Also Results in Changes in the Fluorescence Trace, Suggesting Changes in the Conformation of the pG·R·CCUCUϵA Ternary Complex.* A thio substitution for the *pro-*R_p phosphoryl oxygen atom at the site of phosphoryl transfer (Figure 1) results in an enhancement and quenching of fluorescence when a preformed complex of the ribozyme and this substrate is mixed with 5 mM pG (Figure 7A). The trace fits best to three exponential phases with the enhancement and first phase of the quenching having rates similar to those of the phosphodiester substrate. The rate of transesterification measured with this phosphorothioate substrate with a ^{32}P assay is 0.05 s^{-1} (data not shown), consistent with the rate of the faster phase of the quenching reporting the rate of the rate-limiting step for phosphoryl transfer. The final slow-quenching transient observed upon excitation at 310 nm could represent an interaction between CCUCUϵA and a differently conformed ribozyme population, photobleaching of CCUCUϵA or the pGϵA product, or a rearrangement of the ribozyme−product complex such as release of pGϵA. Similar slow transients are observed in the absence of ribozyme for all the phosphodiester substrates, for both phosphorothioate substrates, and for pGϵA.

A thio substitution for the *pro-*S_p phosphoryl oxygen atom at the site of phosphoryl transfer results only in a quenching of fluorescence when a preformed complex of the ribozyme and this substrate is mixed with pG (Figure 7B). With a ^{32}P assay, this substrate is observed to react negligibly over the same time course that gives almost complete reaction of the *pro-*R_p phosphorothioate substrate (data not shown). Efficient phosphoryl transfer with the *pro-*R_p and not the *pro-*S_p phosphorothioate is consistent with previous observations (Rajagopal et al., 1989; Piccirilli et al., 1993; McSwiggen & Cech, 1989). Substitution of 1 mM $MnC1_2$ and 4 mM $MgC1_2$ for 5 mM $MgC1_2$ does not restore the rate of transesterification of the *pro-*S_p phosphorothioate to a value close to that for the *pro-*R_p phosphorothioate. Nor does Mn^{2+} "rescue" conformation in binding of this substrate as no enhancement of fluorescence is observed in fluorescence-detected stopped-flow studies (data not shown). An inability of Mn^{2+} to restore the rate of cleavage for this phosphorothioate substrate has been previously observed (Piccirilli et al., 1993; McConnell & Cech, 1995).

Upon mixing the ribozyme and an excess of CCUCUϵA, an exponential enhancement of fluorescence is observed. A plot of τ^{-1} for this enhancement as a function of the concentration of CCUCUϵA reveals a rate increasing with the concentration of CCUCUϵA (Figure 8A). A linear fit

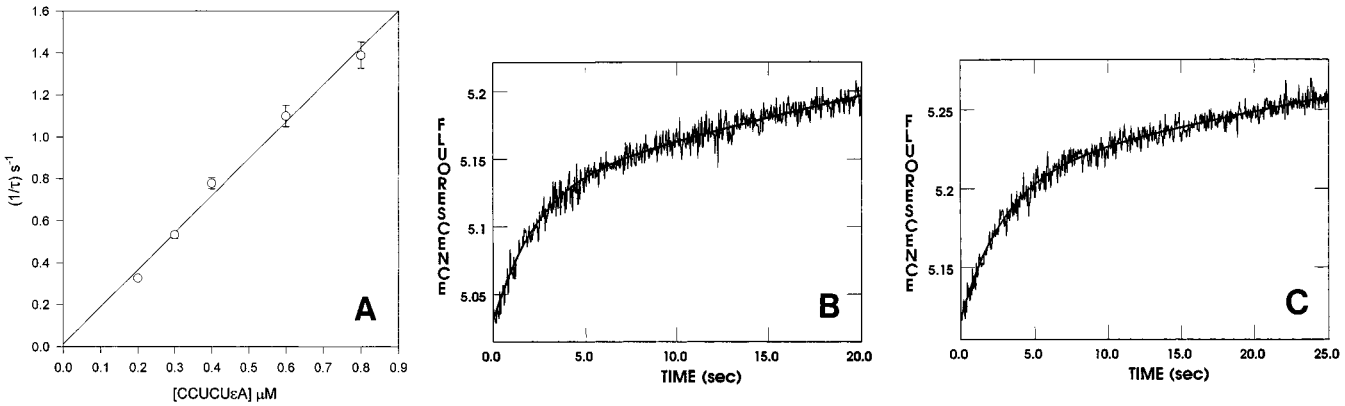

FIGURE 8: (A) Dependence of the observed rate constant for the exponential phase of fluorescence enhancement (τ^{-1}), as described in the text, on concentration of CCUCUϵA. The final concentration of the ribozyme was 50 nM. The solid line represents a linear fit of data. Error bars represent the standard error of the rate. (B) Representative trace and exponential fit for the dependence of fluorescence intensity on time after mixing equal volumes of 500 nM CCUCUϵA, with a *pro-*R_p thio substitution as described in the text, and 100 nM ribozyme. Excitation was at 280 nm. The trace represents an average of three individual traces. The trace is fit to $Y = A_1e^{-k_1t} + k_2t + C$. The observed rate constant of the exponential phase of enhancement is 0.442 ± 0.020 s^{-1}, and the amplitude of enhancement is -0.103 ± 0.002 V. The observed rate of the linear phase of enhancement is $0.003\,20 \pm 0.000\,13$ s^{-1}. Errors are standard errors. $C = 5.133$ V. χ^2 is 0.0217. (C) Representative trace and exponential fit for the dependence of fluorescence intensity on time after mixing equal volumes of 500 nM CCUCUϵA, with a *pro-*S_p thio substitution as described in the text, and 100 nM ribozyme. Excitation was at 280 nm. The trace represents an average of two individual traces. The trace is fit to $Y = A_1e^{-k_1t} + k_2t + C$. The observed rate constant of the exponential phase of enhancement is 0.335 ± 0.013 s^{-1}, and the amplitude of enhancement is -0.0926 ± 0.0016 V. The observed rate constant of the linear phase of enhancement is $0.001\,92 \pm 0.000\,08$ s^{-1}. Errors are standard errors. $C = 5.210$ V. χ^2 is 0.0127.

of this plot yields a slope of $1.8 \times 10^6 \pm 0.1 \times 10^6$ M^{-1} s^{-1} and an intercept of 0.02 ± 0.05 s^{-1}. Since these rates are consistent with the rates of 4.4×10^6 M^{-1} s^{-1} and 0.016 s^{-1} for association and dissociation, respectively, of base pairing between pyrene-CCUCUA and the ribozyme (Bevilacqua et al., 1994), this fluorescence transient presumably reports formation of helix P1 between ribozyme and CCUCUϵA. Mixing the ribozyme with the *pro-*R_p or *pro-*S_p phosphorothioate results in an enhancement of fluorescence similar to that of the phosphodiester in terms of rate and amplitude at similar concentrations of each substrate and ribozyme (Figure 8B,C). Thus both the *pro-*R_p and *pro-*S_p phosphorothioates bind to the ribozyme. For each of the three substrates, a linear increase in fluorescence follows the exponential phase of the enhancement. A similar linear increase in fluorescence, without the initial exponential phase, is observed when CCUCUϵA is mixed with buffer alone. Therefore, this transient is attributed to an effect, e.g. photochemistry, on the excess substrate which is not bound to ribozyme.

DISCUSSION

Fluorescent substrates provide a way to follow individual steps in assembly of the catalytic site of the *Tetrahymena* ribozyme. For example, the dynamics of splice site docking into the catalytic core have been followed with substrates labeled at the 5′ end with pyrene (Bevilacqua et al., 1992, 1994; Li et al., 1995; Turner et al., 1996). Here, we show that the fluorescence of a splice site substrate labeled with the much smaller ϵA probe at the 3′ end is sensitive to binding of G substrates. Rapid mixing experiments with this fluorescent substrate and its phosphorothioate derivatives provide insights into the steps required for G binding and into the importance of the 2′-OH group of G and the nonbridging, *pro-*S_p phosphoryl oxygen atom at the site of phosphoryl transfer for productive alignment of the splice site for reaction.

Binding of G substrates involves at least two steps, since the rate of the fluorescence enhancement reporting pG binding exhibits a hyperbolic dependence on pG concentration. Also, pdG induces no change in fluorescence even though it binds. Evidently, the fluorescence enhancement observed with pG is dependent on a conformational rearrangement following initial binding, and this conformational rearrangement is dependent on the 2′-OH group of pG. Thus, the two-step binding shown in Scheme 1 is the minimal mechanism consistent with the available observations.

For the mechanism in Scheme 1, the first step is G substrate binding to the preformed R·CCUCUϵA complex, presumably at the previously characterized G substrate binding site (Figure 1B) (Michel et al., 1989; Yarus et al., 1991; Yarus & Majerfeld, 1992). This bimolecular step is a rapid pre-equilibrium so that the measured rate constants for binding are apparent bimolecular association rate constants, $k_{on,app} = k_2k_1/k_{-1}$, for the G substrates completing both steps in binding. For Scheme 1, the kinetic data provide rate constants of 0.6 and 0.8 s^{-1} for k_{-2} with pG and GUCG, respectively, consistent with both substrates being trapped by a similar conformational change following initial binding. This conformational change enhances binding of pG and GUCG by approximately 7- and 15-fold, respectively. Other deconvolutions of the measured rates for a two-step binding mechanism are possible, but would require coincidences in combinations of rate constants between pG and GUCG. Therefore, Scheme 1 and the calculated rate constants (Table 1) represent a reasonable model for the dynamics of binding of pG and GUCG.

It has previously been shown that, under identical solution conditions, docking of a pyrene-labeled 5′ splice site analogue into the catalytic core of the L-21 *Sca*I ribozyme requires the binding of a G substrate (Bevilacqua et al., 1994). Thus, it is probable that the second step in binding of CCUCUϵA involves docking of the 5′ splice site analogue into the catalytic core of the ribozyme. The docking and undocking rate constants for the pyrene-labeled 5′ splice site

analogue, pyrene-CCUCUA, are 0.60 and 0.15 s^{-1}, respectively, similar to the values of 4.2 and 0.6 s^{-1} measured here for k_2 and k_{-2}, respectively, of CCUCUϵA (Table 1). This is consistent with both pairs of rate constants arising from docking of the 5′ splice site analogue. Furthermore, enhanced binding of pG, by 7-fold, in the second step in binding is consistent with the cooperativity observed between binding of pG and CCCUCUA (McConnell et al., 1993). In that study, binding of pG enhanced by a factor of 5 was observed, but only in the presence of a docked 5′ splice site analogue. As will be discussed, the docking rearrangements observed with both ϵA and pyrene depend on the 2′-OH of pG, also suggesting that these rearrangements are similar. Thus, the results with two very different fluorescent probes suggest the rate constants for helix docking and undocking in this system are on the order of 1 s^{-1}. These are fundamental steps in RNA folding and unfolding. The rate constants are several orders of magnitude slower than rate constants for formation of secondary structure under similar conditions (Yuan et al., 1979; Labuda et al., 1984). Rate constants for rupture of secondary structure range from faster to slower depending on the sequence (Turner et al., 1990). Thus, it is possible for a tertiary interaction associated with helix docking to stabilize and "capture" a secondary structure before the secondary structure has time to unfold.

2′-dG is a competitive inhibitor of G in transesterification catalyzed by the *Tetrahymena* intron (Bass & Cech, 1986). Both pdG and GUCdG bind approximately as tightly as their all-ribo counterparts to the *Tetrahymena* ribozyme but do not participate in transesterification (Moran et al., 1993). The similar binding of GUCdG and GUCG is confirmed here (Table 1). The 2′-OH could be crucial for reaction because it affects the catalytic step or because it has a specific role in assembling the docked ternary complex of the 5′ splice site, G substrate, and ribozyme in preparation for transesterification, or both. Spectroscopic results presented here reveal a role for the 2′-OH in assembling the ternary complex. Upon binding of pG or GUCG to a preformed complex of the fluorescent 5′ splice site analogue, CCUCUϵA, and ribozyme, an enhancement of fluorescence is observed. No enhancement of fluorescence and a quenching of fluorescence are observed, however, upon binding of pdG and GUCdG, respectively. A fluorescence inversion is also observed upon substituting pdG for pG with the fluorescent 5′ splice site analogue pyrene-CCUCUA (Li & Turner, 1997). These differences in fluorescence imply that a differently conformed ternary complex of the 5′ splice site, G substrate, and ribozyme is produced in the presence of the 2′-H compared to that in the presence of the 2′-OH. The presence of the 2′-H could either disfavor docking or result in a docked state without the proper alignment for catalysis. The 2′-H could also perturb a conformational rearrangement following the docking step. In this case, the fluorescence enhancement detected with CCUCUϵA and pG would arise from an additional rearrangement of the ternary complex after the docking step and before phosphoryl transfer. In support of this possibility is the fact that pdG and GUCdG bind approximately as tightly as their all-ribo counterparts. That is, these deoxy-G substrates may undergo two binding steps, but their 2′-H groups may not promote this subsequent rearrangement, a repositioning that does not significantly alter binding stability. Thus, the spectroscopic probe provides more than just binding information. It indicates that the final conformation is different in the presence or absence of the terminal 2′-OH of the G substrate, even though the binding constant is essentially the same. Thus, the catalytic rate could be negligible because the fraction of bound substrate in a required intermediate state is negligible. A function for the 2′-OH of G in binding and/or positioning of the 5′ splice site could explain the observation of Emerick and Woodson (1994), who found that GTP, but not dGTP, induces a conformational rearrangement of the *Tetrahymena* RNA precursor which leads to splicing of the intron.

Binding with a 3′-H on a 3′dG substrate contrasts with that for a 2′-H on a dG substrate. As with GUCG, GUC3′dG induces an enhancement of fluorescence upon binding to R· CCUCUϵA. This implies that GUC3′dG produces a docked ternary complex with a conformation similar to that with GUCG.

Similarities in the rates and amplitudes of fluorescence enhancements observed upon mixing the ribozyme with CCUCUϵA phosphodiester, *pro*-R_p phosphorothioate, or *pro*-S_p phosphorothioate suggest that each substrate binds to the ribozyme in the absence of pG with similar stabilities and conformations. This enhancement presumably reports base pairing between these ϵA-labeled substrates and the internal guide sequence of the ribozyme for forming helix P1. Upon addition of pG to these base-paired complexes of the ribozyme and substrate, however, fluorescence traces obtained with the *pro*-S_p phosphorothioate differ from those obtained with the *pro*-R_p phosphorothioate (Figure 7) or the phosphodiester. The *pro*-R_p phosphorothioate produces an enhancement and quenching of fluorescence with rates and amplitudes similar to those obtained with the phosphodiester. Rates measured for transesterification with a ^{32}P assay are also similar for these two substrates. These results suggest that sulfur at the *pro*-R_p position does not interfere with positioning of substrates and transesterification. However, no enhancement of fluorescence and a negligible transesterification rate are obtained when pG is mixed with a preformed complex of the ribozyme and the *pro*-S_p phosphorothioate. Previous results have demonstrated that a *pro*-S_p sulfur inhibits reaction (Rajagopal et al., 1989; Piccirilli et al., 1993), but the mechanism for this inhibition remains unknown (Piccirilli et al., 1993; McConnell & Cech, 1995). Our results suggest a mechanism for inhibition whereby, like the 2′-H on pdG, sulfur at the *pro*-S_p position induces an altered conformation of the ternary complex of pG, the ribozyme, and the 5′ splice site analogue which inhibits the phosphoryl transfer step. Although a steric effect with the larger sulfur might lead to altered binding, a hydrogen bond or coordination with a metal ion is more likely compromised in the presence of sulfur. Since both the *pro*-S_p sulfur and the 2′-H on pdG affect the same binding rearrangement in similar ways, it is possible that these two groups interact with one another. For example, as suggested by Turner et al. (1996), the 2′-OH of pG could align the phosphodiester bond for transesterification by forming a hydrogen bond to a nonbridging oxygen, in this case the *pro*-S_p oxygen, in much the same way that the OH group of a tyrosine positions the reactive phosphodiester bond in the exonuclease site of Klenow fragment (Freemont et al., 1988; Beese & Steitz, 1991). Indirect association of the two sites via a water, metal ion, or ribozyme group would also be possible (Sugimoto et al., 1988, 1989; Sjögren et al., 1997; Toh et al., 1987).

Interestingly, the conformational rearrangement reported by the fluorescence quenching equilibrates approximately 10-fold faster with GUCG than with pG. As previously discussed, the rate of the conformational rearrangement reported by the fluorescence quenching represents the limiting rate for transesterification with pG. For GUCG, this faster rate could be due to a faster rate for a conformational rearrangement ordered prior to or concomitant with the bond cleavage event of transesterification. The presence of helix P9.0, formed by the additional UC nucleotides (Figure 1B), could alter helix packing and the orientation of GUCG at the catalytic core, leading to a faster equilibration rate for this conformational rearrangement.

ACKNOWLEDGMENT

The authors thank Dr. Philip Bevilacqua for helpful comments on the manuscript.

SUPPORTING INFORMATION AVAILABLE

Four figures reporting τ_e^{-1} and τ_q^{-1} vs concentrations of pG and GUCG (4 pages). Ordering information is given on any current masthead page.

REFERENCES

Banerjee, A. R., & Turner, D. H. (1995) *Biochemistry 34*, 6504−6512.
Bass, B. L., & Cech, T. R. (1986) *Biochemistry 25*, 4473−4477.
Bates, P. J., Dosanjh, H. S., Kumar, S., Jenkins, T. C., Laughton, C. A., & Neidle, S. (1995) *Nucleic Acids Res. 23*, 3627−3632.
Beese, L. S., & Steitz, T. A. (1991) *EMBO J. 10*, 25−33.
Bernasconi, C. F. (1976) *Relaxation Kinetics*, Chapter 4, Academic Press, New York.
Bevilacqua, P. C., Kierzek, R., Johnson, K. A., & Turner, D. H. (1992) *Science 258*, 1355−1358.
Bevilacqua, P. C., Johnson, K. A., & Turner, D. H. (1993) *Proc. Natl. Acad. Sci. U.S.A. 90*, 8357−8361.
Bevilacqua, P. C., Li, Y., & Turner, D. H. (1994) *Biochemistry 33*, 11340−11348.
Crothers, D. M., Cole, P. E., Hilbers, C. W., & Shulman, R. G. (1974) *J. Mol. Biol. 87*, 63−88.
Emerick, V. L., & Woodson, S. A. (1994) *Proc. Natl. Acad. Sci. U.S.A. 91*, 9675−9679.
Fersht, A. (1985) *Enzyme Structure and Mechanism*, 2nd ed., W. H. Freeman and Co., New York.
Freemont, P. S., Friedman, J. M., Beese, L. S., Steitz, T. A., & Sanderson, M. R. (1988) *Proc. Natl. Acad. Sci. U.S.A. 85*, 8924−8928.
Herschlag, D., & Cech, T. R. (1990a) *Biochemistry 29*, 10159−10171.
Herschlag, D., & Cech, T. R. (1990b) *Biochemistry 29*, 10172−10180.
Herschlag, D., Piccirilli, J. A., & Cech, T. R. (1991) *Biochemistry 30*, 4844−4854.
Hilbers, C. W., Robillard, G. T., Shulman, R. G., Blake, R. D., Webb, P. K., Fresco, R., & Riesner, D. (1976) *Biochemistry 15*, 1874−1882.
Inoue, T., & Kay, P. S. (1987) *Nature 327*, 343−346.
Iyer, R. P., Egan, W., Regan, J. B., & Beaucage, S. L. (1990) *J. Am. Chem. Soc. 112*, 1253−1254.
Johnson, K. A. (1986) *Methods Enzymol. 134*, 677−705.
Kay, P. S., & Inoue, T. (1987) *Nucleic Acids Res. 15*, 1559−1577.
Kubota, Y., Motoda, Y., Fujisaki, Y., & Steiner, R. F. (1983) *Biophys. Chem. 18*, 225−232.
Labuda, D., Striker, G., & Pörschke, D. (1984) *J. Mol. Biol. 174*, 587−604.
Latham, J. A., & Cech, T. R. (1989) *Science 245*, 276−282.
Le Cuyer, K. A., & Crothers, D. M. (1994) *Proc. Natl. Acad. Sci. U.S.A. 91*, 3373−3377.
Li, Y., & Turner, D. H. (1997) *Biochemistry 36*, 11131−11139.
Li, Y., Bevilacqua, P. C., Mathews, D., & Turner, D. H. (1995) *Biochemistry 34*, 14394−14399.
Maher, L. J., III, Dervan, P. B., & Wold, B. (1990) *Biochemistry 29*, 8820−8826.
Markiewicz, W. T., Biala, E., & Kierzek, R. (1984) *Bull. Pol. Acad. Sci., Chem. 32*, 433−451.
McConnell, T. S., & Cech, T. R. (1995) *Biochemistry 34*, 4056−4067.
McConnell, T. S., Cech, T. R., & Herschlag, D. H. (1993) *Proc. Natl. Acad. Sci. U.S.A. 90*, 8362−8366.
McSwiggen, J. A., & Cech, T. R. (1989) *Science 244*, 679−683.
Michel, F., & Westhof, E. (1990) *J. Mol. Biol. 216*, 585−610.
Michel, F., Hanna, M., Green, R., Bartel, D. P., & Szostak, J. W. (1989) *Nature 342*, 391−395.
Moran, S., Kierzek, R., & Turner, D. H. (1993) *Biochemistry 32*, 5247−5256.
Piccirilli, J. A., Vyle, J. S., Caruthers, M. H., & Cech, T. R. (1993) *Nature 361*, 85−88.
Rajagopal, J., Doudna, J. A., & Szostak, J. W. (1989) *Science 244*, 692−694.
Rougée, M., Faucon, B., Mergny, J. L., Barcelo, F., Giovannangeli, C., Montenay-Garestier, T., & Hélène, C. (1992) *Biochemistry 31*, 9269−9278.
Sclavi, B., Woodson, S., Sullivan, M., Chance, M. R., & Brenowitz, M. (1997) *J. Mol. Biol. 266*, 144−159.
Shindoe, H., Torigoe, H., & Akinori, S. (1993) *Biochemistry 32*, 8963−8969.
Sjögren, A.-S., Pettersson, E., Sjöberg, B.-M., & Strömberg, R. (1997) *Nucleic Acids Res. 25*, 648−653.
Spencer, R. D., Weber, G., Tolman, G. L., Barrio, J. R., & Leonard, N. J. (1974) *Eur. J. Biochem. 45*, 425−429.
Stec, W. J., Zon, G., Egan, W., & Stec, B. (1984) *J. Am. Chem. Soc. 106*, 6077−6079.
Sugimoto, N., Kierzek, R., & Turner, D, H. (1988) *Biochemistry 27*, 6384−6392.
Sugimoto, N., Tomka, M., Kierzek, R., Bevilacqua, P. C., & Turner, D. H. (1989) *Nucleic Acids Res. 17*, 355−371.
Toh, H., Imamura, A., & Kanada, K. (1987) *FEBS Lett. 219*, 279−282.
Tolman, G. L., Barrio, J. R., & Leonard, N. J. (1974) *Biochemistry 13*, 4869−4878.
Turner, D. H., Sugimoto, N., & Freier, S. M. (1990) in *Nucleic Acids* (Saenger, W., Ed.) Vol. 1C, pp 201−227, Springer-Verlag, Berlin.
Turner, D. H., Li, Y., Fountain, M., Profenno, L., & Bevilacqua, P. C. (1996) *Nucleic Acids Mol. Biol. 10*, 19−32.
Tuschl, T., Gohlke, C., Jovin, T. M., Westhof, E., & Eckstein, F. (1994) *Science 266*, 785−789.
Walter, N. G., & Burke, J. M. (1997) *RNA 3*, 392−404.
Weeks, K. M., & Cech, T. R. (1995) *Biochemistry 34*, 7728−7738.
Yang, M., Ghosh, S. S., & Millar, D. P. (1994) *Biochemistry 33*, 15329−15337.
Yarus, M., & Majerfeld, I. (1992) *J. Mol. Biol. 225*, 945−949.
Yarus, M., Illangesekare, M., & Christian, E. (1991) *J. Mol. Biol. 222*, 995−1012.
Yuan, R. C., Steitz, J. A., Moore, P. B., & Crothers, D. M. (1979) *Nucleic Acids Res. 7*, 2399−2418.
Zarrinkar, P. P., & Williamson, J. R. (1994) *Science 265*, 918−924.
Zaug, A. J., Grosshans, C. A., & Cech, T. R. (1988) *Biochemistry 27*, 8924−8931.

BI9708895